WATER RESOURCES RESEARCH, VOL. 49, 4971–4984, doi:10.1002/wrcr.20385, 2013

Adjoint modeling of stream depletion in groundwater-surface water systems

S. A. Griebling[1,2] and R. M. Neupauer[1]

Received 3 July 2012; revised 18 June 2013; accepted 22 June 2013; published 12 August 2013.

[1] Groundwater pumping may lead to reduction in surface water flows, which can compromise water supplies and habitat. In light of these threats, the need to minimize stream depletion, defined as the reduction in the flow rate in streams and rivers caused by groundwater pumping, becomes paramount. We develop adjoint equations to calculate stream depletion due to aquifer pumping. We consider a coupled groundwater and surface water system in which both the river head and river flow rate are impacted by drawdown in the aquifer as a result of pumping. Through an illustrative example, we show that the adjoint method for calculating stream depletion produces accurate results if the model is approximately linear. With only one simulation of the adjoint equations, stream depletion can be calculated for pumping at a well at any location in the model domain, which results in a substantial reduction in computational time as compared to the standard method of calculating stream depletion.

Citation: Griebling, S. A., and R. M. Neupauer (2013), Adjoint modeling of stream depletion in groundwater-surface water systems, *Water Resour. Res.*, *49*, 4971–4984, doi:10.1002/wrcr.20385.

1. Introduction

[2] Stream depletion is the reduction in the flow rate in a river as a result of pumping in an aquifer that is hydraulically connected to the river. Stream depletion has many negative consequences, such as reduction in water supply for municipal, agricultural, and domestic uses; failure to satisfy existing water rights; and destruction of the ecosystems that depend on streams and rivers. Quantifying stream depletion therefore is crucial for protecting water supplies, surface water rights, and environments that depend on the streams and rivers.

[3] Various analytical and semianalytical expressions have been developed to quantify stream depletion for simple systems. *Theis* [1941] and *Glover and Balmer* [1954] presented expressions for calculating stream depletion due to pumping in a two-dimensional, homogeneous, infinite aquifer for a fully penetrating, infinitely long, straight stream that is in perfect hydraulic connection with the aquifer. Later studies developed analytical expressions that relaxed many of these assumptions, including partial hydraulic connection between the river and aquifer [*Hantush*, 1965], time-varying pumping rates [*Jenkins*, 1968; *Wallace et al*., 1990], partially penetrating stream [*Hunt*, 1999; *Butler et al*., 2001], leakage across a confining unit [*Butler et al*., 2007; *Zlotnik and Tartakovsky*, 2008], and a two-layered system with confined and unconfined aquifers [*Hunt*, 2009].

[4] *Sophocleous et al*. [1995] compared the analytical solution of *Glover and Balmer* [1954] to results of numerical simulations and found that the most restrictive assumptions of Glover and Balmer's model are perfect hydraulic connection between the stream and aquifer, full penetration of the stream, and a homogeneous aquifer; thus, analytical solutions have limitations. While analytical solutions are easy to apply, they are only applicable for idealized cases, and numerical models are necessary to simulate stream depletion in more complicated systems.

[5] The standard approach for using numerical models to calculate stream depletion is to first run one groundwater flow simulation without pumping to determine the exchange of water between the river and the aquifer, and then to run an additional simulation with pumping at one location to determine the change in the flow rate of water between the river and the stream. If the location of a new well is to be chosen, many possible well locations may be under consideration. It may be necessary to choose a location that limits depletion in a nearby stream; therefore, stream depletion must be calculated for many different well locations. Assuming the aquifer is sufficiently complex to require numerical models to simulate stream depletion, the standard approach must be repeated for each potential well location, and can become computationally inefficient if many potential well locations are considered. *Neupauer and Griebling* [2012] presented an adjoint method for calculating stream depletion in a river due to pumping in an adjacent aquifer. With the adjoint method, only one simulation is needed to calculate stream depletion for a well at

Additional supporting information may be found in the online version of this article.

[1]Department of Civil, Environmental, and Architectural Engineering, University of Colorado Boulder, Boulder, Colorado, USA.
[2]Now at Headwaters Corporation, Denver, Colorado, USA.

Corresponding author: R. M. Neupauer, Department of Civil, Environmental, and Architectural Engineering, University of Colorado Boulder, 1111 Engineering Dr., Boulder, CO 80309, USA. (neupauer@colorado.edu)

0043-1397/13/10.1002/wrcr.20385

any location in the aquifer; thus it is more efficient than the standard approach when multiple potential well locations are considered.

[6] The goal of this paper is to present the adjoint method for calculating stream depletion for a fully coupled river and aquifer system, in which both the aquifer head and the river head are affected by pumping in the aquifer. This model is a more realistic model of surface water and groundwater interaction than has been used previously with the adjoint method. *Neupauer and Griebling* [2012] developed the adjoint model assuming that the river head was known and was independent of the head in the aquifer. That model is simplistic because stream depletion, by definition, leads to changes in the flow rate and therefore to changes in the head in the river. For that model, both the forward and adjoint equations have the same form, so the adjoint equations can be solved using a standard groundwater flow code.

[7] In the next section, we present the forward equations of groundwater and stream flow, and we provide a mathematical expression for stream depletion. With our fully coupled river and aquifer system, the forward model is nonlinear. Next, we develop the adjoint equations for this stream and aquifer system, and we discuss the approach for solving the adjoint equations using a standard groundwater flow code. Because of the nonlinearity of the forward model, the adjoint equations do not have the same form as the forward equations; thus a standard groundwater flow code must be modified to solve the adjoint equations. In our adjoint derivation, we include tributaries and evapotranspiration, which were not included in previous work on adjoint methods for calculating stream depletion. Finally, we present an example of using the adjoint method to calculate stream depletion; we use these results to investigate the importance of various system parameters on stream depletion; and we demonstrate that the adjoint method is accurate and requires substantially less computation time than the standard approach.

2. Forward Equations of Flow and Stream Depletion

[8] We consider a system with an unconfined aquifer that is separated from a confined aquifer by a leaky aquitard. We use the Dupuit approximation in the unconfined aquifer. We assume horizontal flow in the confined aquifer and vertical flow in the aquitard, and we neglect aquitard storage. A river and one or more tributaries partially penetrate the unconfined aquifer. We consider natural recharge and evapotranspiration in the unconfined aquifer, and precipitation, evaporation, and lateral inflows in the river and tributaries. We assume that transient changes in storage in the river and tributaries are fast relative to the seepage across the bed sediments; therefore, we neglect transient changes in the river and tributary volumes. This assumption is consistent with commonly used groundwater flow models such as the Stream package [*Prudic*, 1989] in MODFLOW-2000 [*Harbaugh et al*., 2000]. MODFLOW, along with its associated river and stream packages, has been used in numerous case studies that calculate stream depletion [e.g., *Myers et al*., 1996; *Leake et al*., 2005, 2010; *Peterson et al*., 2008; *Leake and Pool*, 2010; *Stanton et al*., 2010; *Lambert et al*., 2011]. Thus, an adjoint approach based on the assumptions used in MODFLOW has potential for widespread use.

[9] In this work, we define a tributary as any segment of a river whose downstream terminus is a confluence with another river segment, while the term river is reserved for the segment whose downstream terminus is the model domain boundary. In the notation used below, tributaries are numbered $k = 1, 2 \ldots N-1$, where $N-1$ is the number of tributaries, the river is denoted as Tributary $k=N$, and d_k denotes the tributary that is downstream of tributary k. For example, in Figure 1, Tributaries 1 and 2 flow into Tributary 3 (river), so $d_1 = d_2 = 3$. We define $\mathcal{D}_k = \{m | d_m = k\}$ to denote the set of all d for which $d_m = k$. For this hydraulic system, the governing equations for flow in the unconfined aquifer, confined aquifer, and tributaries and river, respectively, are given by

$$S_y \frac{\partial h_u}{\partial t} = \nabla \cdot [\mathbf{K}(h_u - \zeta)\nabla h_u] - Q_{pu}\delta(\mathbf{x} - \mathbf{x}_w) + N_R(\mathbf{x}) - E_T(\mathbf{x}) - \frac{K_a}{b_a}(h_u - h_c) + \sum_{k=1}^{N} \frac{K_k}{b_k}(h_k - h_u)B_k(\mathbf{x}) \tag{1}$$

$$S \frac{\partial h_c}{\partial t} = \nabla \cdot [\mathbf{T}\nabla h_c] - Q_{pc}\delta(\mathbf{x} - \mathbf{x}_w) + \frac{K_a}{b_a}(h_u - h_c), \tag{2}$$

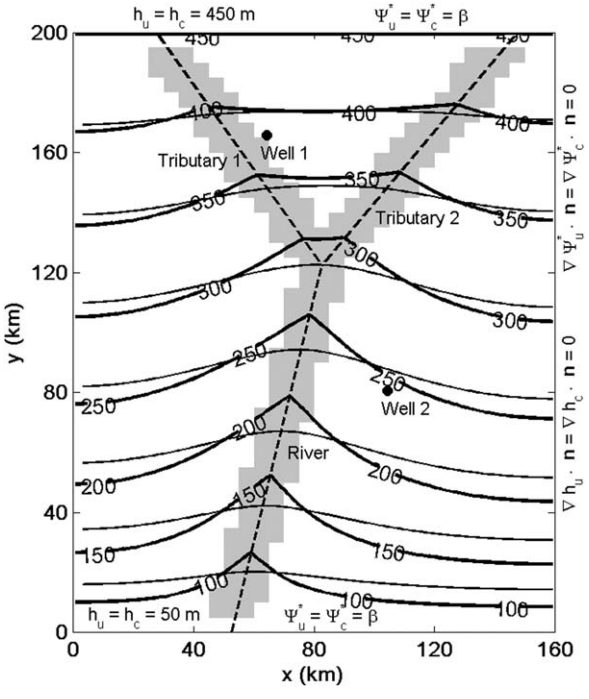

Figure 1. Model domain. Contours represent head (m) in the unconfined aquifer (thick line) and in the confined aquifer (thin line). Thick dashed lines represent tributaries and rivers. Boundary conditions for the forward and adjoint models are shown along the boundaries (the same boundary conditions are used at $x = 0$ km and at $x = 160$ km). Gray shaded region represents area where evapotranspiration is occurring. The two filled circles represent the two well locations used in Figure 7.

$$\frac{\partial Q_k}{\partial s_k} = -\frac{K_k}{b_k}(h_k - h_u)w_k + Pw_k - Ew_k + I'_{Lk}, k = 1, 2, \ldots N, \tag{3}$$

where h_u and h_c are the heads in the unconfined and confined aquifers, respectively, $\mathbf{x} = (x,y)$ is the position vector in the horizontal plane, t is time, S_y is specific yield, S is storage coefficient, $\mathbf{K}$ is the hydraulic conductivity tensor for the unconfined aquifer, $\mathbf{T}$ is the transmissivity tensor for the confined aquifer, ζ is the elevation of the bottom of the unconfined aquifer, $h_u - \zeta$ is the saturated thickness of the unconfined aquifer, $N_R(\mathbf{x})$ is the natural recharge rate, $E_T(\mathbf{x})$ is the evapotranspiration rate from the aquifer, Q_{pu} and Q_{pc} are the pumping rates for a well in the unconfined and confined aquifers, respectively, $\mathbf{x}_w = (x_w, y_w)$ is the location of a pumping well, $\delta(\cdot)$ is the Dirac delta function, K_a and b_a are the hydraulic conductivity and thickness, respectively, of the aquitard, K_k and b_k are the hydraulic conductivity and thickness, respectively, of the bed sediment of tributary k, h_k is head in tributary k, $B_k(\mathbf{x})$ is a dimensionless function that has a value of unity at tributary k and a value of zero elsewhere, A_k, Q_k, and w_k are the cross-sectional area, flow rate, and width, respectively, of tributary k, s_k is the spatial coordinate in the flow direction along the channel of tributary k, P is precipitation, E is the evaporation rate from the river and tributaries, and I'_{Lk} are the lateral inflows per unit length along tributary k.

[10] Although evapotranspiration depends on vegetation type, meteorological conditions, and other variables, we adopt a simplified model of the evapotranspiration rate, E_T, as follows. If aquifer head is above a threshold head, h_s, evapotranspiration occurs at the maximum rate, E_{Tmax}. If aquifer head is below $h_s - d$, where d is the extinction depth, evapotranspiration is negligible. For aquifer heads between $h_s - d$ and h_s, the evapotranspiration rate varies linearly from zero to E_{Tmax}. Mathematically, this dependence can be expressed as

$$E_T = \frac{E_{Tmax}}{d}[(h_u - h_s + d)H(h_u - h_s + d) - (h_u - h_s)H(h_u - h_s)], \tag{4}$$

where $H(\cdot)$ represents the Heavyside function. This evapotranspiration model is used in the evapotranspiration package in MODFLOW [*Harbaugh et al.*, 2000].

[11] Let the boundary and initial conditions on the governing equations be defined as

$$h_u(\mathbf{x}, t) = g_{1u}(\mathbf{x}, t) \text{on } \Gamma_{1u}, \tag{5}$$

$$\nabla h_u \cdot \mathbf{n} = g_{2u}(\mathbf{x}, t) \text{on } \Gamma_{2u}, \tag{6}$$

$$\alpha_u h_u(\mathbf{x}, t) - \mathbf{K}\nabla h_u \cdot \mathbf{n} = g_{3u}(\mathbf{x}, t) \text{on } \Gamma_{3u}, \tag{7}$$

$$h_u(\mathbf{x}, 0) = h_{u0}, \tag{8}$$

$$h_c(\mathbf{x}, t) = g_{1c}(\mathbf{x}, t) \text{on } \Gamma_{1c}, \tag{9}$$

$$\nabla h_c \cdot \mathbf{n} = g_{2c}(\mathbf{x}, t) \text{on } \Gamma_{2c}, \tag{10}$$

$$\alpha_c h_c(\mathbf{x}, t) - \mathbf{T}\nabla h_c \cdot \mathbf{n} = g_{3c}(\mathbf{x}, t) \text{on } \Gamma_{3c}, \tag{11}$$

$$h_c(\mathbf{x}, 0) = h_{c0}, \tag{12}$$

$$Q_k(s_k = 0, t) = \begin{cases} Q'_k(t) & \text{if } \mathcal{D}_k = \varnothing \\ \sum_{m \in \mathcal{D}_k} Q_m(s_m = L_m, t) & \text{otherwise} \end{cases}, \tag{13}$$

where $g_{ij}(\mathbf{x}, t)$ is a known function, Γ_{ij} is an aquifer boundary, $i = 1, 2, 3, j = u, c$, where u denotes the unconfined aquifer and c denotes the confined aquifer, α_u and α_c are known constants that depend on the physical properties of the boundary, $\mathbf{n}$ is the outward unit normal vector, h_{u0}, h_{c0}, and h_{k0} are the initial heads in the unconfined aquifer, confined aquifer, and tributary k respectively, Q'_k is the flow rate at the upstream boundary of tributary k, and L_k is the length of tributary k. The upstream boundary of the tributaries are specified flux boundaries that either are equal to the sum of the outflows from segments that flow into the tributary (such as for Tributary 3 (river) in Figure 1) or are specified (such as for Tributary 1 in Figure 1).

[12] We assume that the river and tributaries have a wide, rectangular cross-section, and we assume that the relationship between flow rate and river head is described by Manning's equation, which, for a wide, rectangular channel, is given by

$$Q_k \approx \frac{c}{n_k} S_{ok}^{1/2} w_k (h_k - z_k)^{5/3}, \tag{14}$$

where $c = 86{,}400$ s/d is the number of seconds in a day, z_k is the channel bottom elevation, $h_k - z_k$ is the flow depth, n is Manning's roughness coefficient (in units of s/m$^{1/3}$), and S_o is the channel bottom slope.

[13] Stream depletion, $\Delta Q_N(L_N, t_c)$, is the decrease in the river flow rate at a compliance point L_N and compliance time t_c, resulting from pumping. It can be obtained by first solving equations (1)–(3) with equations (5)–(13) with no pumping to determine $Q_N(L_N, t_c)$ in the absence of pumping; then repeating the simulation with pumping at a single well to determine $Q_N(L_N, t_c)$ with pumping. Finally, stream depletion is calculated as the difference between these two values of $Q_N(L_N, t_c)$. If stream depletion is desired for pumping wells at other locations, one additional simulation must be run for each pumping well location. Below, we present an alternative approach that permits the calculation of stream depletion for a well at any location in the aquifer by performing only a single simulation of an adjoint model.

[14] For small pumping rates, stream depletion is linearly proportional to the pumping rate and can be expressed mathematically as

$$\Delta Q_N(L_N, t_c) \approx -\frac{dQ_N(L_N, t_c)}{dQ_{pj}} Q_{pj}, \tag{15}$$

where the derivative on the right-hand side represents the sensitivity of the river flow rate to the pumping rate. Rearranging equation (3), $Q_N(L_N, t_c)$ can be expressed as

$$Q_N(L_N, t_c) = Q_N(s_N = 0, t_c) - \int_0^{L_N} \left\{ w_N \left[\frac{K_N}{b_N}(h_N - h_u)|_{t=t_c} - P + E \right] - I'_{LN} \right\} ds_N. \tag{16}$$

[15] Using this equation and recognizing that precipitation, evaporation, and lateral inflows are independent of pumping, we write the sensitivity of the river flow rate to the pumping rate as

$$\frac{dQ_N(L_N,t_c)}{dQ_{pj}} = \frac{dQ_N(s_N=0,t_c)}{dQ_{pj}} - \int_0^{L_N}\left\{w_N\frac{K_N}{b_N}(\psi_N-\psi_u)|_{t=t_c}\right\}ds_N, \quad (17)$$

where $\psi_u = \partial h_u/\partial Q_{pj}$ and $\psi_N = \partial h_N/\partial Q_{pj}$, are the marginal sensitivities of head to the pumping rate. The first term on the right-hand side is the sensitivity of the inflow into the river to the pumping rate. Since this inflow comes from the tributaries, for which equations similar to equation (17) can be written, the iterative application of equation (17) to the river and the tributaries yields

$$\frac{dQ_N(L_N,t_c)}{dQ_{pj}} = -\sum_{k=1}^{N}\left[\int_0^{L_k}\left\{w_k\frac{K_k}{b_k}(\psi_k-\psi_u)|_{t=t_c}\right\}ds_k\right], \quad (18)$$

where $\psi_k = \partial h_k/\partial Q_{pj}$.

[16] Substituting equation (18) into equation (15), we obtain a new expression for stream depletion, given by

$$\Delta Q_N(L_N,t_c) \approx Q_{pj}\int_\Omega\sum_{k=1}^{N}\left[\frac{K_k}{b_k}(\psi_k-\psi_u)|_{t=t_c}B_k(\mathbf{x})\right]d\mathbf{x}, \quad (19)$$

where $w_k ds_k = B_k(\mathbf{x})d\mathbf{x}$, and Ω is the spatial domain. The sensitivity equation in (19) forms the basis of the derivation of the adjoint equation.

3. Adjoint Equations and Stream Depletion

[17] To avoid having to solve equations (1)–(3) once for each possible well location to calculate stream depletion due to pumping from many different wells, we develop the adjoint equivalent to those governing equations. Ultimately, we want to calculate the stream depletion from equation (19), which depends on the marginal sensitivities of aquifer head and tributary head to pumping rate. These marginal sensitivities can be calculated by solving equations similar to the forward equations (1)–(3); however, these equations can be solved only for a single pumping well location at a time. Thus, the system of equations would have to be solved once for each possible well location. To avoid this limitation, we rewrite the sensitivity equation (19) in terms of new variables, the adjoint states, and the resulting expression for stream depletion becomes (see supporting information)

$$\Delta Q_N(L_N,t_c) \approx Q_{pj}\int_0^{t_c}\psi_j^*(\mathbf{x},\tau)d\tau, \quad (20)$$

for pumping from a well at any location $\mathbf{x}$ in aquifer j ($j=u$ for unconfined and $j=c$ for confined), where $\tau = t_c - t$ is backward time, and ψ_u^* and ψ_c^* are adjoint states of head in the unconfined and confined aquifers, respectively, that satisfy the following adjoint equations (see derivation in supporting information)

$$S_y\frac{\partial\psi_u^*}{\partial\tau} = \nabla\cdot\left[\mathbf{K}(h_{uo}-\zeta)\nabla\psi_u^*\right] - \frac{K_a}{b_a}\left(\psi_u^*-\psi_c^*\right) + \sum_{k=1}^{N}\frac{K_k}{b_k}\left(\psi_k^*-\psi_u^*\right)B_k(\mathbf{x}) - \frac{E_{Tmax}\psi_u^*}{d}\left[H(h_u-h_s+d)-H(h_u-h_s)\right] \quad (21)$$

$$S\frac{\partial\psi_c^*}{\partial\tau} = \nabla\cdot\left[\mathbf{T}\nabla\psi_c^*\right] + \frac{K_a}{b_a}\left(\psi_u^*-\psi_c^*\right) \quad (22)$$

$$-\frac{\partial}{\partial s_k}\left(\frac{5c}{3}\frac{S_{ok}^{1/2}w_k}{n_k}(h_{ko}-z_k)^{2/3}\psi_k^*\right) = -\frac{K_k}{b_k}\left(\psi_k^*-\psi_u^*\right)w_k - \psi_k^*\frac{5c}{3}\frac{\partial}{\partial s_k}\left(\frac{S_{ok}^{1/2}w_k}{n_k}(h_{ko}-z_k)^{2/3}\right) \quad \text{for } k=1,2,\ldots N, \quad (23)$$

where ψ_k^* is the adjoint state of head in tributary k. The initial conditions are given by (see supporting information)

$$\psi_u^*(x,y,\tau=0) = \sum_{k=1}^{N}\frac{K_k}{b_k S_y}B_k(\mathbf{x}) \quad (24)$$

$$\psi_c^*(x,y,\tau=0) = 0. \quad (25)$$

[18] The boundary conditions on the adjoint states are given by (see supporting information)

$$\psi_u^*(\mathbf{x},\tau) = 0 \text{ on } \Gamma_{1u}, \quad (26)$$

$$\nabla\psi_u^*\cdot\mathbf{n} = 0 \text{ on } \Gamma_{2u}, \quad (27)$$

$$\alpha_u\psi_u^*(\mathbf{x},\tau) - \mathbf{K}\nabla\psi_u^*\cdot\mathbf{n} = 0 \text{ on } \Gamma_{3u}, \quad (28)$$

$$\psi_c^*(\mathbf{x},\tau) = 0 \text{ on } \Gamma_{1c}, \quad (29)$$

$$\nabla\psi_c^*\cdot\mathbf{n} = 0 \text{ on } \Gamma_{2c}, \quad (30)$$

$$\alpha_c\psi_c^*(\mathbf{x},\tau) - \mathbf{T}\nabla\psi_c^*\cdot\mathbf{n} = 0 \text{ on } \Gamma_{3c}. \quad (31)$$

$$\psi_N^*(s_N=L_N,\tau) = 0, \quad (32)$$

$$\psi_k^*(s_k=L_k,\tau) = \psi_{d_k}^*(s_{d_k}=0,\tau) \quad \text{for } k=1,2,\ldots N-1. \quad (33)$$

[19] To calculate stream depletion for a well at any location in either the unconfined or confined aquifer, the adjoint equations (21)–(23) are solved once and the results are used in equation (20) to calculate stream depletion. Since a single simulation of the adjoint equations calculates the adjoint state at any $\mathbf{x}$ in the domain, only one adjoint simulation is needed to calculate stream depletion caused by pumping at a well at any location in the aquifer.

[20] The adjoint equations (21)–(23) are similar in form to the forward equations (1)–(3); therefore a code that solves the forward equations, such as MODFLOW, can be adapted to solve the adjoint equations. See Appendix A for additional information on solving the adjoint equations with MODFLOW. Note, however, that there are a few key differences between the forward and adjoint equations:

[21] 1. The state variables in the forward equations are head, which have units of length; the state variables in the adjoint equations are adjoint states, which have units of reciprocal time.

[22] 2. The time variable in the forward equation is forward time, while the time variable in the adjoint equation is

Table 1. Parameter Values for the Aquifers and Aquitard

Parameter	Value	Range[a]
Top elevation of unconfined aquifer (m)	500	Variable
Bottom elevation of unconfined aquifer (m)	0	Variable
Top elevation of confined aquifer (m)	−50	Not present
Bottom elevation of confined aquifer (m)	−100	Not present
Specific yield, S_y	0.2	0.01–0.3
Hydraulic conductivity in unconfined aquifer, K (m/d)	50	3–60
Natural recharge rate, N_R (m/d)	1.5×10^{-4}	$0–2\times10^{-4}$
Maximum evapotranspiration rate, E_{Tmax} (m/d)	6×10^{-4}	$2.5\times10^{-4}–1\times10^{-3}$
Extinction depth for evapotranspiration, d (m)	1.5	1.5
Hydraulic conductivity of aquitard, K_a (m/d)	5×10^{-5}	Not present
Specific storage in confined aquifer, S (m^{-1})	3×10^{-5}	3×10^{-5}
Transmissivity of confined aquifer, T (m^2/d)	500	Not present
Pumping rate (m^3/d)	2.5×10^{-4}	2500
Compliance time, t_c (years)	50	50
Spatial domain size (km)	160 × 200	400 × 260
Spatial discretization (km)	1.25 × 1.25	3 × 3
β (d^{-1})	450	Not applicable
γ	1×10^{-8}	Not applicable

[a]From *Peterson et al*. [2008].

backward time; thus, in the adjoint simulation, information is propagated backward in time.

[23] 3. Several load terms from the forward equation do not appear in the adjoint equations because they are insensitive to pumping; these include aquifer recharge, and precipitation, evaporation, and lateral inflows to the tributaries and river.

[24] 4. The pumping term in the forward equation does not appear in the adjoint equation. Instead, it appears in the sensitivity equation.

[25] 5. The boundary conditions on the adjoint groundwater equations are homogeneous. The initial conditions are homogeneous, except where the aquifer is adjacent to the river and tributaries.

[26] 6. The groundwater flow term in the forward equation for the unconfined aquifer is nonlinear in head h_u; therefore the related term in the adjoint is linear in the adjoint state but contains the forward state variable, h_u. As an approximation, we assume that the saturated thickness of the unconfined aquifer can be approximated as constant, so we replace the time-dependent saturated thickness $h_u - \zeta$ with $h_{uo} - \zeta$. We treat the unconfined aquifer as if it were a confined aquifer with an effective transmissivity of $\mathbf{K}(h_{uo} - \zeta)$. This assumption is valid under low pumping conditions, which is consistent with the adjoint method developed here.

[27] 7. The adjoint evapotranspiration rate is nonzero only at locations where $h_s - d < h_u < h_s$ in the forward model, and it varies linearly with the adjoint state.

[28] 8. In the forward river and tributary equations, the sign on the flow term is positive; while in the adjoint equations, it is negative. This allows for the upstream propagation of information in the adjoint approach.

[29] 9. In the forward river and tributary equations, the flow term relates flow rate to river head using Manning's equation (14). In the adjoint equation, the flow term relates $\partial Q_k / \partial Q_{pj}$ to the adjoint state; thus the "adjoint flow" in the adjoint equation is given by

$$\frac{\partial Q_k}{\partial Q_{pj}} = \frac{5c}{3}\frac{S_{ok}^{1/2} w_k}{n_k}(h_{ko} - z_k)^{2/3}\psi_k^*. \tag{34}$$

[30] 10. The boundary conditions on the adjoint equation for the river and tributaries are specified adjoint state at the downstream boundary of the river, and continuous adjoint state at the downstream boundaries of the tributaries. The initial conditions depends on K_k/b_k.

[31] 11. The flow term in the forward equation for the river and tributaries is nonlinear in head h_k; therefore the related term in the adjoint is linear in the adjoint state but contains the forward state variable, h_r. As an approximation, we assume that the flow depth of the river and tributaries can be approximated as constant, so we replace the time-dependent flow depth $h_k - z_k$ with $h_{ko} - z_k$.

[32] 12. The adjoint equations for the river and tributaries have an extra load term that depends on the spatial derivatives of S_{ok}, w_k, n_k, and $h_{ko} - z_k$.

4. Example

[33] In this section, we demonstrate the use of the adjoint approach for calculating stream depletion in a synthetic aquifer, and we evaluate the sensitivity of stream depletion to various model parameters. The example aquifer system consists of an unconfined aquifer, a leaky aquitard, and a confined aquifer. Two tributaries and one river are hydraulically connected to the unconfined aquifer, as shown in Figure 1, and flow is in the –y-direction. We calculate stream depletion at the downstream terminus of the river at $t_c = 18{,}250$ days $= 50$ years for pumping at a rate of 2.5×10^4 m^3/d at a single well or a cluster of wells whose locations are represented as the center of any grid block in the unconfined and confined aquifers. The domain geometry and boundary conditions for the aquifers are shown in Figure 1. We chose to use a two-aquifer system to demonstrate that the adjoint method is applicable for pumping in either the confined or unconfined aquifer, and in aquifers that are in direct and indirect (i.e., through a confining layer) hydraulic communication with the river. We chose to use two tributaries to demonstrate that the adjoint method is developed accurately for systems that include a river and its tributaries.

[34] To ensure realistic parameter values for our study, we used parameter values from a groundwater model that was developed to investigate stream depletion due to

Table 2. Parameter Values for the Tributaries and River

Parameter	Tributary 1	Tributary 2	River
Upstream coordinates (km)	(27.5,200.0)	(147.5,200.0)	(0.825,122.5)
Downstream coordinates (km)	(0.825,122.5)	(0.825,122.5)	(0.525,0.0)
Manning's roughness coefficient, n_k	0.04	0.04	0.04
Channel width, w_k (m)	5	7	12
Channel bottom elevation, z_k, at upstream (m)	448.0	448.07	269.0
Channel bottom elevation, z_k, at downstream (m)	269.0	269.0	42.0
Channel bottom slope, S_{ok}	1.88×10^{-3}	1.77×10^{-3}	1.8077×10^{-3}
Bed sediment thickness, b_k (m)	0.3	0.3	0.3
Bed sediment hydraulic conductivity, K_k (m/d)	0.14	0.15	0.09
Conductance parameter, $K_k w_k/b_k$ (m/d)	2.3	3.5	3.6
Head at upstream boundary (m)	446.60	447.23	calculated
Discharge at upstream boundary (m^3/d)	2155	326,000	calculated

irrigation pumping (among other objectives) in the unconfined aquifer in the Elkhorn and Loup River Basins in Nebraska [*Peterson et al*., 2008]. Because our domain geometry and our two-aquifer system does not match the physical system of the Elkhorn and Loup River Basin aquifers, we are not attempting to reproduce the model results of *Peterson et al*. [2008]; we are simply using their model parameter values as guidance for selecting physically realistic parameter values for our synthetic aquifer system. Aquifer parameter values used in this study, and ranges of the parameter values reported in *Peterson et al*. [2008], where available, are shown in Table 1. River parameter values used in this study are reported in Table 2. Most river parameters were not reported directly in *Peterson et al*. [2008]; however, they reported a bed sediment thickness of 1 ft ($\approx$ 0.3 m) and a calibrated river conductance, defined as $K_k w_k/b_k$, ranging from 0.06 to 9.6 m/d. For these parameters, we used values within their ranges; for other parameters, we chose reasonable values.

[35] We use MODFLOW-2000 with the Stream (STR) package [*Prudic*, 1989] to solve the forward and adjoint equations. The STR package assumes that the tributaries and rivers have a wide rectangular channel cross-section. Also, the STR package assumes that the transient change in river and tributary volumes can be neglected, consistent with equation (3). For simplicity, we assume precipitation, evaporation, and lateral inflows are negligible in the river and tributaries; thus, $P = E = I_L^{'} = I_{Lk}^{'} = 0$. This assumption is not necessary for using the adjoint model.

[36] The first step in solving the adjoint equations for stream depletion is to solve the forward equations for aquifer and river head in the absence of pumping. The head distribution in these aquifers in the absence of pumping is shown in Figure 1. Head increases in the $+y$-direction. Table 3 shows the inflow and outflow rates and the upstream and downstream heads and flow depths for each tributary and river in the absence of pumping. The increase in flow rate between the upstream and downstream boundaries of each tributary and the river demonstrate that both tributaries and the river are gaining.

[37] To calculate stream depletion, we ran MODFLOW-2000 with the adjoint version of the STR package [*Griebling*, 2012] to obtain the adjoint states. Since the form of the adjoint river and tributary equation (23) is different than the form of the forward equation (3), some modifications to the STR code were necessary to solve the adjoint equation; these changes are described in *Griebling* [2012]. The head distribution in the unconfined aquifer in the absence of pumping was used to determine the effective transmissivity of the unconfined aquifer in the adjoint model, and to determine where the adjoint evapotranspiration rate is nonzero (i.e., where $h_s - d < h_u < h_s$).

[38] The adjoint states obtained from the adjoint simulation were used in equation (20) to calculate stream depletion. The results are shown in Figures 2a and 2b for the unconfined and confined aquifers, respectively. For a given location in the model domain, these plots show the amount of stream depletion in the downstream terminus of the river after 18,250 days (50 years) of pumping at the given location. The results show that stream depletion is highest for wells near the tributaries and river, while stream depletion decreases as the distance between the well and the tributary or river increases. If a well is near the tributaries or river, high drawdown occurs in the aquifer beneath the tributaries or river, which leads to lower exchange of water from the aquifer to the tributaries and river for these gaining reaches, and therefore leads to a reduction in flow rate in the river, i.e., stream depletion. If a well is far from the tributaries or river, less drawdown occurs near the tributaries and river, resulting in less stream depletion. In this case, a higher proportion of the pumped water comes from flow across the constant head boundaries of the model.

[39] For comparison, we also calculated stream depletion using the standard approach. In this example, each grid block in the unconfined and confined aquifers was considered to be a potential well location, for a total of 40,960 potential well locations, which would require 40,960 forward simulations to obtain the same information as is

Table 3. Tributary and River Flow Conditions in the Absence of Pumping

Parameter	Tributary 1	Tributary 2	River
Head at upstream boundary (m)	446.60	447.23	271.21
Head at downstream boundary (m)	272.73	272.83	46.41
Flow depth at upstream boundary (m)	0.04	0.67	2.35
Flow depth at downstream boundary (m)	2.27	2.37	3.25
Discharge at upstream boundary (m^3/d)	2155	326,000	4,554,000
Discharge at downstream boundary (m^3/d)	1,846,000	2,708,000	7,857,000

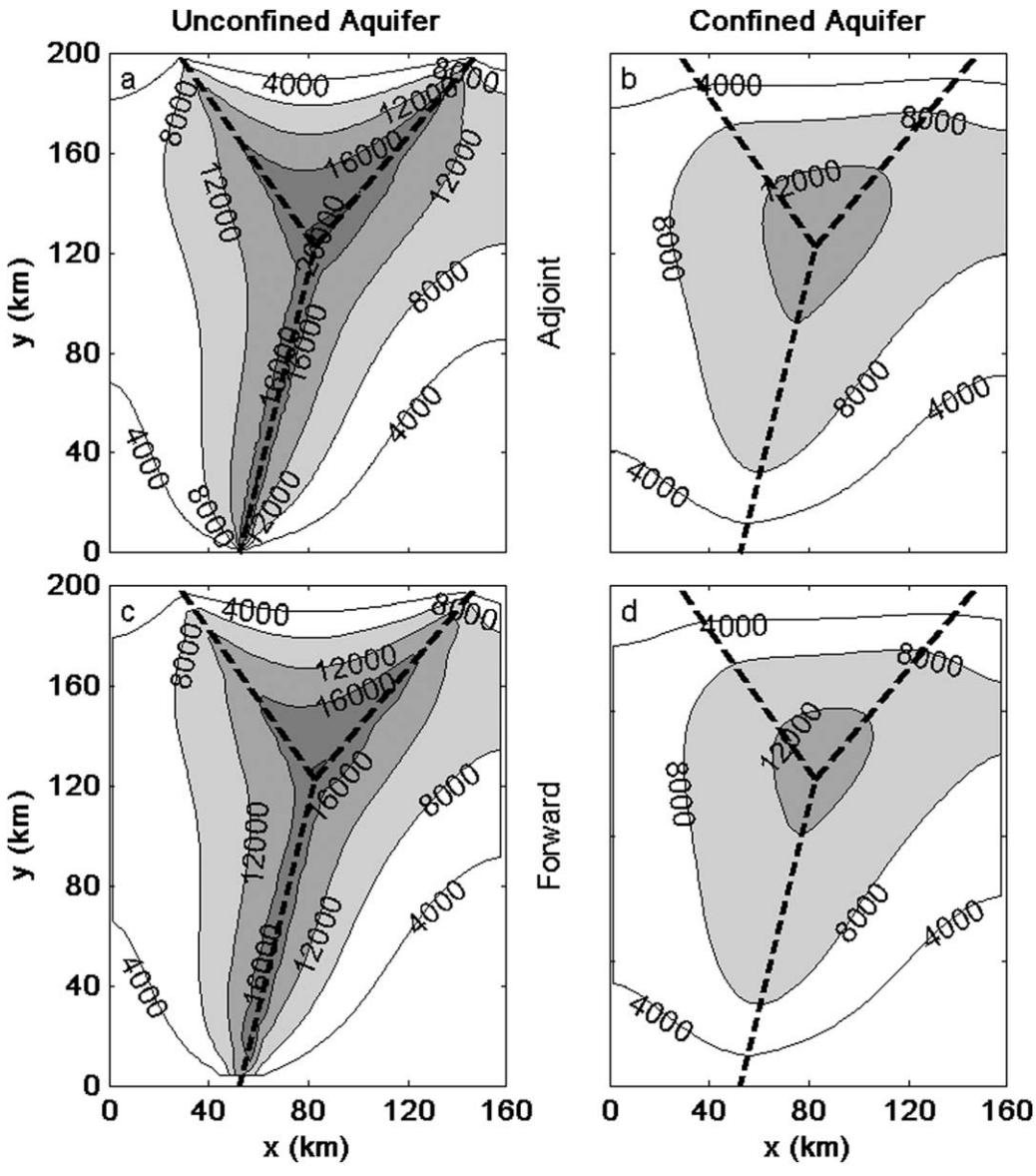

Figure 2. Stream depletion (m^3/d) in the river due to pumping in the (left column) unconfined and (right column) confined aquifers, calculated using (top row) one adjoint simulation and (bottom row) multiple forward simulations. Thick dashed lines represent tributaries and rivers. The pumping rate used in these simulations is 2.5×10^4 m^3/d.

obtained from one adjoint simulation. Instead of considering every cell as a potential well location, we considered the cells at the intersection of every fourth row and every fourth column as potential well locations, for a total of 2560 potential well locations. The results are shown in Figures 2c and 2d. Comparison with Figures 2a and 2b shows that the adjoint simulation produces very similar results as the standard approach. For both aquifers, the patterns are very similar between the results of the two methods, with some slight variations near the tributaries and rivers. Figure 3 shows the percent difference between the stream depletion values calculated for the adjoint and forward simulations. The differences are between 0 and 4% throughout most of the domain, except where the stream depletion is low. In these areas, the absolute error is low.

5. Discussion

5.1. Sensitivity Analysis

[40] To analyze the effects of various parameters on stream depletion, we ran additional simulations each with one parameter value modified. Figures 4a and 4d show stream depletion for pumping in the unconfined and confined aquifers, respectively, when the hydraulic conductivity of the river and tributary bed sediment, K_k, is reduced by a factor of two. Comparison of the results with the base case scenario in Figures 2a and 2b shows that a reduction in K_k leads to a reduction in stream depletion. With a lower value of bed sediment hydraulic conductivity, flow between the river and aquifer is impeded; thus more of the pumped water is drawn from across the model boundaries and less from the stream.

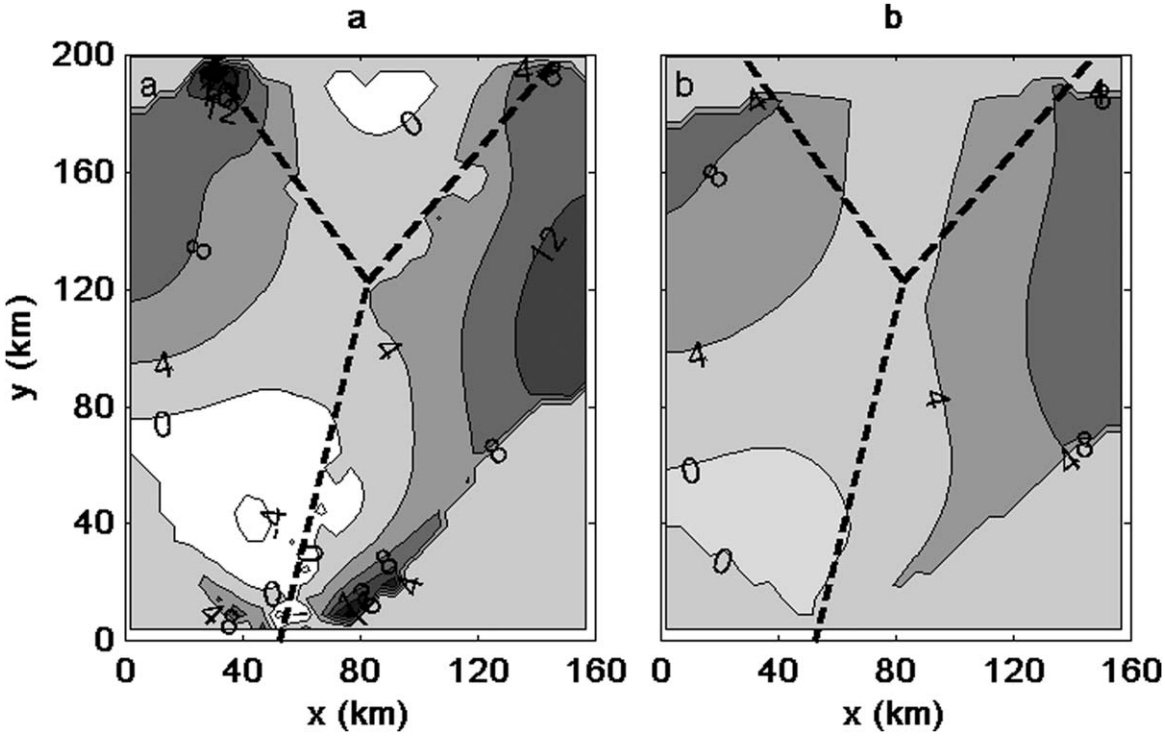

Figure 3. Percent difference in stream depletion values calculated using the adjoint method and the standard method in the (a) unconfined aquifer and (b) confined aquifer. Wherever stream depletion exceeds 4000 m^3/d, the value is set to zero. Thick dashed lines represent tributaries and rivers.

[41] Figures 4b and 4e show stream depletion when the maximum evapotranspiration rate, E_{Tmax}, is doubled relative to the base case in Figures 2a and 2b. An increase in E_{Tmax} leads to a reduction in stream depletion. Recall that in the evapotranspiration model used here (equation (4)), as aquifer head decreases, the evapotranspiration rate, E_T, decreases at a rate proportional to E_{Tmax}. Thus for a higher value of E_{Tmax}, E_T decreases at a higher rate, resulting in less water removed by evapotranspiration and more available in aquifer storage relative to the base case. Water that was removed by evapotranspiration in the base case is available to be pumped, and stream depletion decreases.

[42] Figures 4c and 4f show stream depletion when the aquitard hydraulic conductivity, K_a, is reduced by a factor of two. Stream depletion due to pumping in the unconfined aquifer is essentially unchanged relative to the base case (compare Figures 2a and 4c), because K_a has little effect on flow in the unconfined aquifer. On the other hand, the magnitude of K_a has a significant effect on stream depletion due to pumping in the confined aquifer (compare Figures 2b and 4f). With a lower value of K_a, there is less hydraulic communication between the confined aquifer, where the well is pumping, and the unconfined aquifer, which is in hydraulic communication with the river; thus, a lower value of K_a leads to less stream depletion due to pumping in the confined aquifer.

[43] To further evaluate the sensitivity of stream depletion to K_a, we simulated stream depletion due to pumping when K_a is decreased by factors of 2 and 10 and increased by factors of 2 and 10. The results are shown in Figure 5 for pumping in the confined aquifer. As expected, a reduction in K_a leads to less stream depletion, and an increase in K_a leads to more stream depletion. For pumping in the unconfined aquifer, the results are visually indistinguishable from the results in Figure 4c, and are not shown here.

[44] We also evaluated the effects of spatially varying K_a on stream depletion. We considered two different Gaussian random K_a fields: one with a mean K_a of $\mu_{K_a} = 5 \times 10^{-6}$ m/d and standard deviation of $\sigma_{K_a} = 1.5 \times 10^{-6}$ m/d, and the other with $\mu_{K_a} = 5 \times 10^{-4}$ m/d and $\sigma_{K_a} = 1.5 \times 10^{-4}$ m/d. We generated one normally distributed random field (shown in Figure 6) with unit variance and a correlation length of 2.5×10^4 m using sequential Gaussian simulation with Geostatistical Software Library (GSLIB) [*Deutsch and Journel*, 1992] with a spherical variogram. To obtain the random K_a fields, we scaled the random field in Figure 6 by the desired standard deviation and added the desired mean.

[45] Stream depletion due to pumping in the confined aquifer for the two random K_a fields is shown in Figure 5c and 5f. For the scenarios evaluated here, stream depletion is sensitive to the mean of the random K_a distribution but is insensitive to the random variations. For example, Figure 5b shows stream depletion due to pumping in the confined aquifer with a homogeneous aquitard with $K_a = 5 \times 10^{-6}$ m/d, and Figure 5c shows stream depletion due to pumping in the confined aquifer with a heterogeneous aquitard mean K_a of 5×10^{-6} m/d. The two plots are visually indistinguishable. As pumping in the confined aquifer produces a cone of depression, vertical flow is induced from the unconfined aquifer into the confined aquifer. The spatially varying aquitard conductivity leads to local variations in

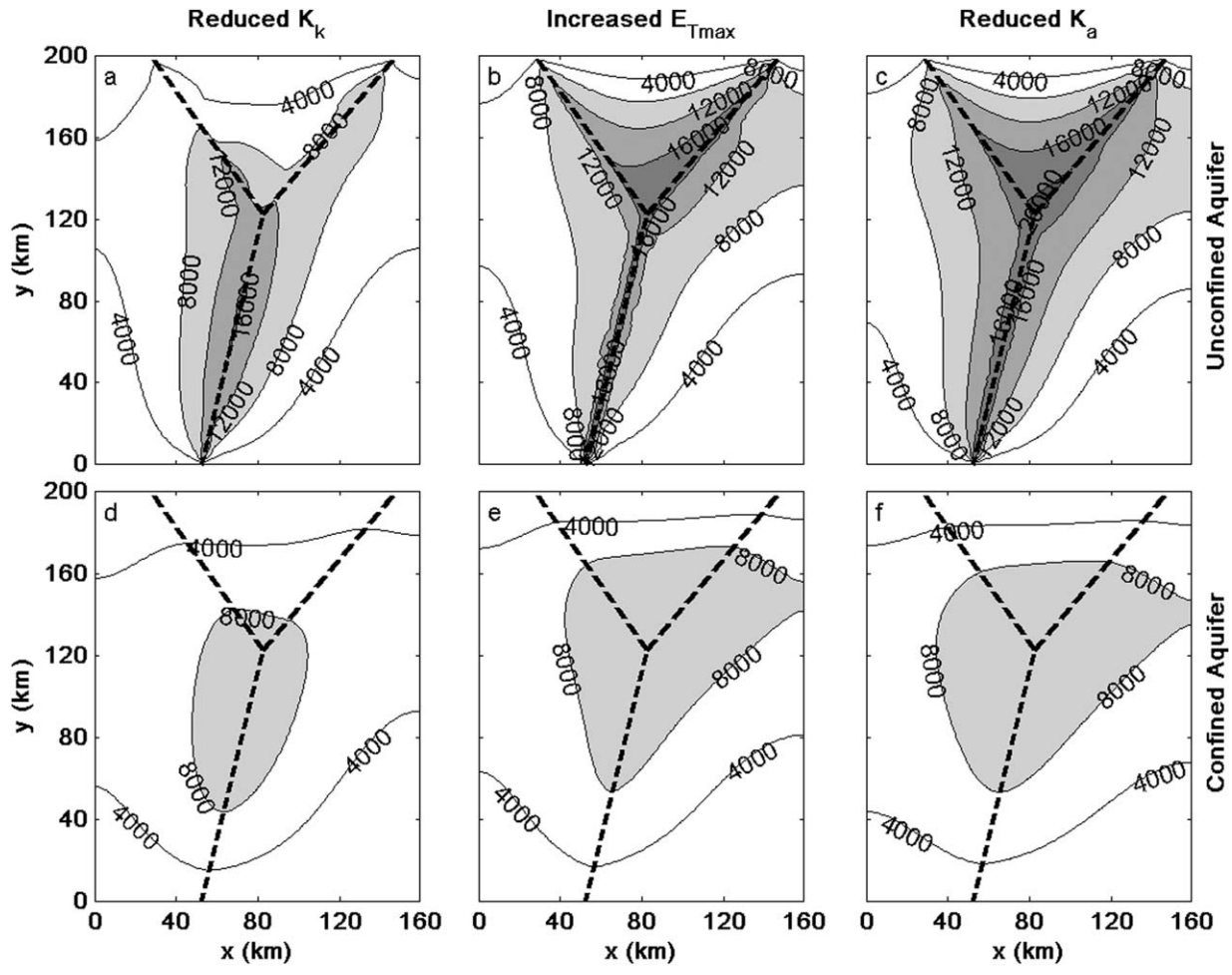

Figure 4. Stream depletion (m^3/d) in the river due to pumping in the (top row) unconfined and (bottom row) confined aquifers, as a result of (left column) reducing K_k, (middle column) increasing E_{Tmax}, and (right column) reducing K_a. Thick dashed lines represent tributaries and rivers.

the vertical flow. Since the cone of depression covers a large spatial extent, the total flow across the aquitard averages out the local variations in vertical flow. Thus, the total flow across the aquitard and therefore the stream depletion are more sensitive to the average aquitard conductivity than to its local spatial variations for the scenarios evaluated here.

5.2. Sources of Error

[46] The adjoint states are related to marginal sensitivities of head to the pumping rate; thus each term in the adjoint equation represents the sensitivity of various processes to the pumping rate. The adjoint derivation requires differentiation of each term of the forward equation with respect to pumping rate. For the nonlinear terms (i.e., $\nabla[\mathbf{K}(h_u - \zeta)\nabla h_u]$, $\partial Q_k/\partial s_k$) and piecewise linear term (i.e., evapotranspiration), these derivatives are linearized around the prepumping conditions. A source of error in the adjoint model as compared to the results of the standard approach is due to this linearization. The transmissivity of an unconfined aquifer depends on the saturated thickness of the aquifer, which can vary over time as the head in the aquifer varies. In a pumping scenario, the head, saturated thickness, and transmissivity would decrease over time. The adjoint approach ignores the time variation of the saturated thickness; thus, the transmissivity used in the adjoint simulation can be higher than the transmissivity used in equivalent forward simulations.

[47] Another potential source of error is in the assumption that stream depletion varies linearly with pumping rate, as shown in equation (15). In the adjoint simulation, we calculate dQ_k/dQ_{pj} and multiply this value by the pumping rate to estimate stream depletion, so the adjoint simulation results are only valid if stream depletion varies linearly with pumping rate. We ran forward simulations for a range of pumping rates ($Q_{pu} = 0$ to 5×10^6 m^3/d) for two different well locations (Wells 1 and 2 in Figure 1) in the unconfined aquifer. Stream depletion caused by this range of pumping rates at each of the wells is shown in Figure 7. Well 1 is closer to the tributary, so drawdown is higher for pumping at Well 1 than for pumping at Well 2, for any given pumping rate. For pumping at either well, stream depletion varies approximately linearly until the simulated pumping rate exceeds a threshold pumping rate above which the model cell containing the well goes dry. If the cell goes dry, pumping ceases in the simulation causing stream depletion to drop and approach zero. This

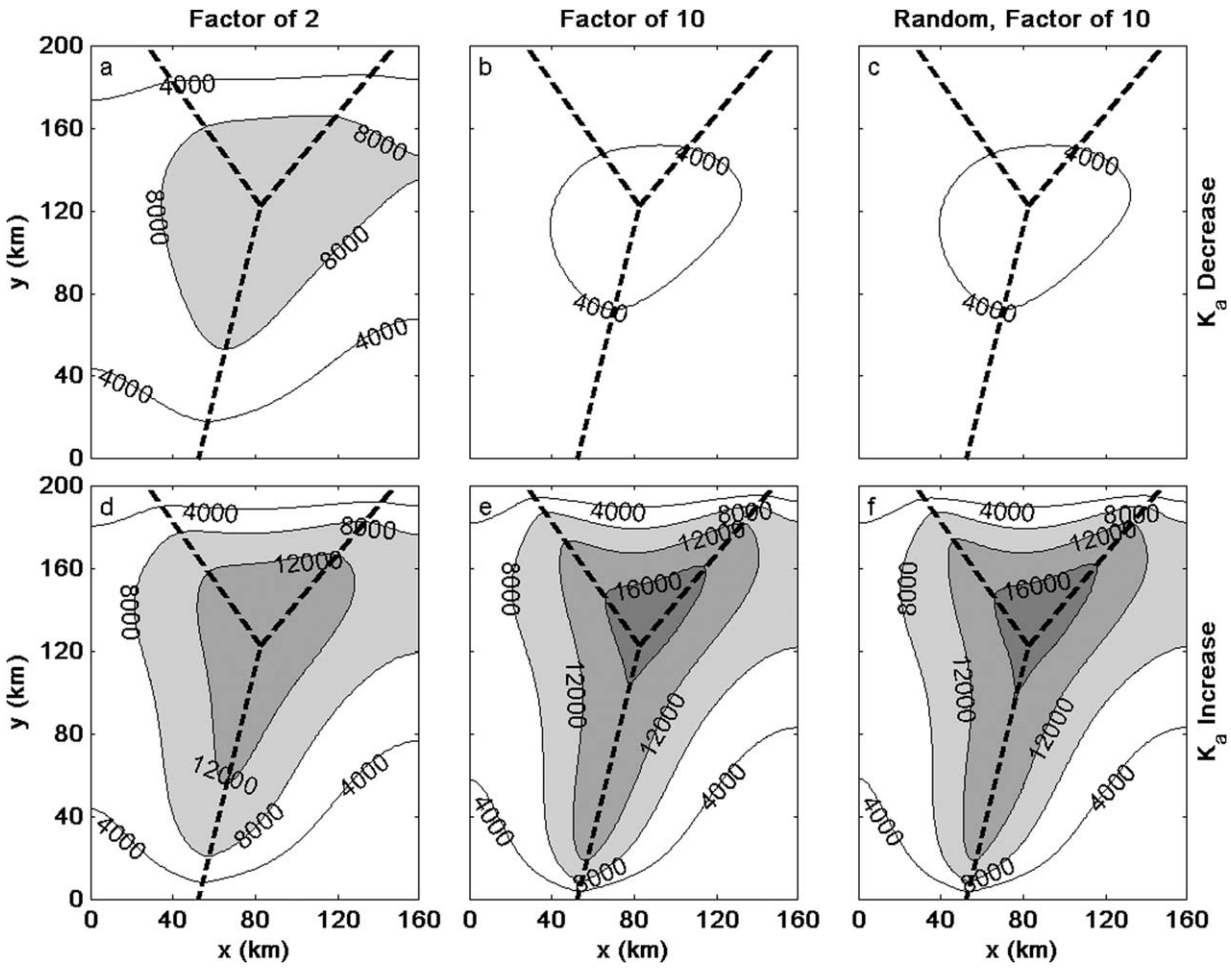

Figure 5. Stream depletion (m^3/d) in the river due to pumping in the confined aquifer with the hydraulic conductivity of the aquitard changed to (a) $K_a = 2.5 \times 10^{-5}$ m/d, (b) $K_a = 5 \times 10^{-6}$ m/d, (c) random K_a field with a mean of 5×10^{-6} m/d and a standard deviation of 1.5×10^{-6} m/d, (d) $K_a = 1 \times 10^{-4}$ m/d, (e) $K_a = 5 \times 10^{-4}$ m/d, and (f) random K_a field with a mean of 5×10^{-4} m/d and a standard deviation of 1.5×10^{-5} m/d. Thick dashed lines represent tributaries and rivers.

threshold pumping rate is higher for Well 1 because the saturated thickness of the aquifer is greater where the head is higher.

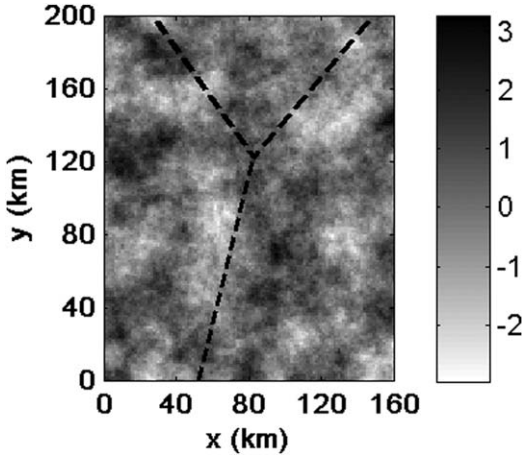

Figure 6. Random field used to generate the random K_a fields. Thick dashed lines represent tributaries and rivers.

[48] For comparison, the adjoint-derived stream depletion is also shown in Figure 7. In the adjoint approach, we calculate a single value of dQ_k/dQ_{pj}, which is the slope of the adjoint stream depletion curves in Figure 7. Thus,

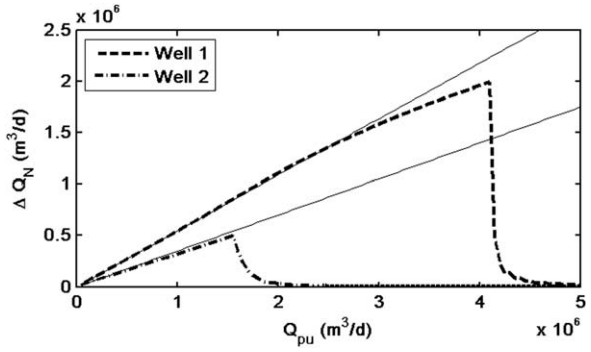

Figure 7. Effects of various pumping rates on stream depletion due to pumping in the two well locations shown in Figure 1. Thin solid lines are the adjoint-based stream depletion estimates.

nonzero stream depletion is calculated even for pumping rates that exceed the well yield. Furthermore, the adjoint stream depletion slightly exceeds the stream depletion calculated from the forward simulations for almost all pumping rates. This discrepancy is likely caused by the assumption in the adjoint approach that the saturated thickness is unchanged during pumping.

[49] In the STR package of MODFLOW, if the aquifer head is above the river channel bottom, the rate of flow across the streambed is proportional to the head difference between the river and the aquifer. However, if the aquifer head drops below the river channel bottom, the rate of flow across the stream bed is proportional to the head difference between the river and the bottom of the bed sediment, where the pressure head is assumed to be zero. Thus, in this case, the flow rate between the river and aquifer is independent of the head in the aquifer, and the river is no longer hydraulically connected to the aquifer. Since the adjoint model only solves for the adjoint state and not for the aquifer head, it is not possible to determine when the river is no longer hydraulically connected to the aquifer. Thus, the adjoint model results are only accurate for pumping scenarios for which the river remains hydraulically connected to the aquifer.

[50] If the adjoint model is used for situations in which stream depletion is not linearly proportional to the pumping rate, the adjoint model results would overestimate stream depletion. Thus, although the results would be inaccurate, they would be conservative.

5.3. Efficiency

[51] The results in Figures 2a and 2b were obtained with one simulation of the adjoint model, which ran in 140 s on a Dell Latitude E6530 with an Intel Core i7–3720QM processor at 2.60 GHz. The adjoint simulation produced stream depletion estimates for a well at any of the 40,960 cells in the model domain, i.e., at 1.25 km × 1.25 km resolution. The results of the standard approach, shown in Figures 2c and 2d, were obtained at 5 km × 5 km resolution (for every fourth model row and every fourth model column), i.e., obtaining 1/16th of the amount of information as obtained from the adjoint simulations. The 2560 forward simulations ran in 582 min, or approximately 250 times longer than the single adjoint simulation.

[52] Prior to running adjoint simulations, it is still necessary to develop and calibrate a forward model of the river and aquifer system. The parameterization of the adjoint model is developed based on the forward model, and the adjoint model requires as input the steady state aquifer head and river head that are obtained from a forward simulation in the absence of pumping. Once the model is developed, the adjoint simulation is more efficient than the standard approach for calculating stream depletion when the number of possible well locations is large.

[53] Typically it is not necessary to obtain stream depletion information for well locations throughout the entire model domain, so the efficiency of the adjoint simulation may be lower than the 250-fold decrease in simulation time seen here. However, for large models with simulation times on the order of multiple hours, the time savings of a single adjoint simulation compared to just 10 or so forward simulations may be substantial. In addition, in performing a sensitivity analysis to calculate the sensitivity of stream depletion to various model parameters, a modeler may want to run simulations with several different parameter sets. Even if the sensitivity is desired for only a small subset of well locations, the computational time for running forward simulations for all combinations well locations and parameter sets may become prohibitive, and the adjoint approach may be more efficient.

5.4. Comparison With Analytical Solutions

[54] Analytical solutions for stream depletion are available for simplified river and aquifer systems. Many of these analytical solutions are straightforward and efficient to calculate, but because they do not account for all of the complexity of the system, they are less accurate than numerical (forward or adjoint) solutions. To illustrate the inaccuracy of analytical solutions, we calculated stream depletion for the unconfined aquifer in our example system using two different analytical solutions. The first is the method of *Glover and Balmer* [1954] which calculates stream depletion as

$$\Delta Q_N = Q_p \operatorname{erfc}\left(\sqrt{\frac{S\ell^2}{4Tt}}\right), \tag{35}$$

where S is the storage property of the aquifer, ℓ is the shortest distance between the well location and the river, T is aquifer transmissivity, and t is time. This method assumes a fully penetrating, infinitely long, straight river in a homogeneous aquifer with negligible change in saturated thickness during pumping. We used this method to calculate stream depletion in the unconfined aquifer, by defining transmissivity as the product of hydraulic conductivity ($K = 50$ m/d) and the average saturated thickness of the aquifer over our model domain ($\overline{h}_u \approx 270$ m). For each position, we calculated the shortest distance to either tributary or the river. The resulting spatial distribution of stream depletion is shown in Figure 8a. This analytical solution clearly overestimates the stream depletion over most of the domain. With the Glover and Balmer method, bed sediment is assumed to have the same hydraulic properties as the aquifer, so water can be pulled as easily from the river as from the surrounding aquifer. In addition, this analytical method does not account for the domain boundaries, partial penetration of the river, evapotranspiration, the spatially variable saturated thickness of the aquifer, and other complexities. This leads to an overestimation of stream depletion, including several locations where all of the pumped water is assumed to be drawn from the river after 50 years of pumping.

[55] The second analytical solution that we evaluated is the method of *Hunt* [1999], which calculates stream depletion as

$$\Delta Q_N = Q_p \left[\operatorname{erfc}\left(\sqrt{\frac{S\ell^2}{4Tt}}\right) - \exp\left\{\frac{\lambda^2 t}{4ST} + \frac{\lambda \ell}{2T}\right\} \operatorname{erfc}\left\{\sqrt{\frac{\lambda^2 t}{4ST}} + \sqrt{\frac{S\lambda^2}{4Tt}}\right\}\right], \tag{36}$$

where $\lambda = K_k w_k / b_k$ and all other parameters are as defined in equation (35). This method accounts for the lower hydraulic conductivity of the bed sediment and does not assume a fully penetrating river. We used this method to

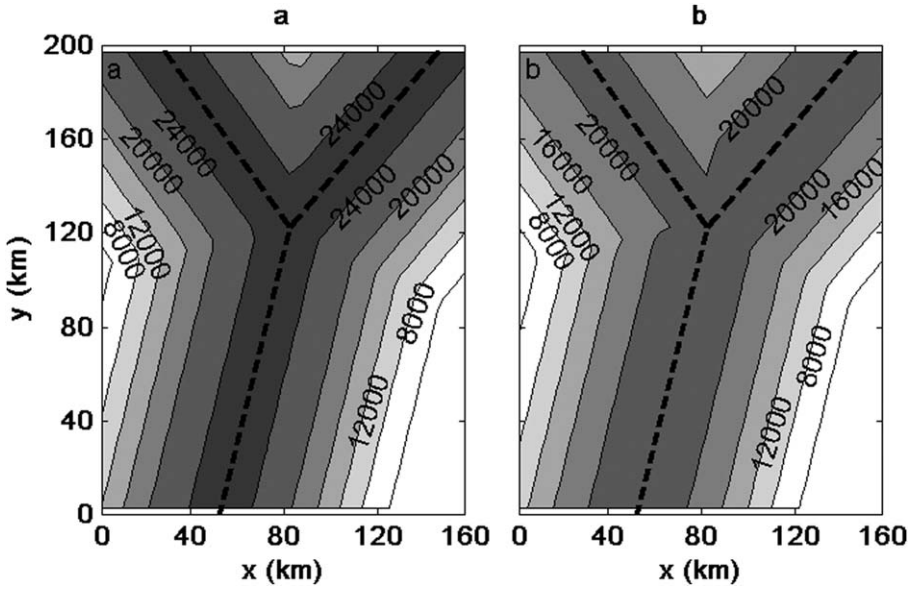

Figure 8. Estimates of stream depletion (m^3/d) in the river due to pumping in the unconfined aquifer using method of (a) *Glover and Balmer* [1954] and (b) *Hunt* [1999]. Thick dashed lines represent tributaries and rivers.

calculate stream depletion in the unconfined aquifer, using the same parameter values as in the Glover and Balmer method. For each position, we used λ for the nearest tributary or river segment. The resulting spatial distribution of stream depletion is shown in Figure 8b. This analytical solution performs better than the Glover and Balmer method. Due to the lower hydraulic conductivity of the bed sediment, water flows more easily through the aquifer than across the bed sediment, so less of the pumped water is drawn from the river. Nevertheless, this method still overestimates stream depletion. Both of these analytical solutions are much less accurate than the adjoint simulation (compare Figures 2a, 8a and 8b).

6. Conclusions

[56] This work develops an adjoint method to calculate stream depletion caused by pumping in an aquifer that is hydraulically connected to a river. Through an illustrative example, we demonstrated the use of MODFLOW-2000 with the stream (STR) package to solve the adjoint equations. The results show that the adjoint solution accurately approximates stream depletion when the assumptions of small changes in river and aquifer head are satisfied. For the example presented here, the difference between the adjoint and forward simulations is small, i.e., <4% of the true value over most of the domain.

[57] We used the adjoint method to determine the sensitivity of stream depletion to several model parameters. We found that stream depletion is sensitive to the hydraulic conductivity of the bed sediments and moderately sensitive to the maximum evapotranspiration rate. For the scenarios evaluated here, we also found that stream depletion due to pumping in the unconfined aquifers is insensitive to the hydraulic conductivity of the aquitard; however, stream depletion due to pumping in the confined aquifer is sensitive to the mean hydraulic conductivity of the aquitard.

[58] The adjoint method is computationally more efficient than the standard method for calculating stream depletion when the number of possible well locations is large. In the example presented here, with 2560 possible well locations considered in the standard approach, the adjoint method was 250 times faster than the standard method. The adjoint method is a useful approach for identifying optimal locations for new wells that minimize stream depletion or for identifying areas along a river section that are most sensitive to pumping.

Appendix A: Solving the Adjoint Equations Using MODFLOW

[59] The adjoint equations can be solved using standard groundwater flow codes, such as MODFLOW, by treating the head variable in the flow code as the adjoint state. Note from equations (26)–(33) that the boundary conditions on the adjoint equations specify that the adjoint states are defined with values of zero, and that the initial conditions in equations (24) and (25) specify an initial value of zero everywhere except at the rivers and tributaries. Since the adjoint state is interpreted as "head" in the groundwater flow code, it is necessary that the magnitude of the adjoint state be greater than the magnitude of the aquifer bottom elevation and the river bottom elevation; otherwise the model will behave as if the aquifer or river is dry. Thus, we define new adjoint states as

$$\Psi_u^*(\mathbf{x},\tau) = \beta + \frac{\psi_u^*(\mathbf{x},\tau)}{\gamma}, \tag{A1}$$

$$\Psi_c^*(\mathbf{x},\tau) = \beta + \frac{\psi_c^*(\mathbf{x},\tau)}{\gamma}, \tag{A2}$$

$$\Psi_k^*(\mathbf{x},\tau) = \beta + \frac{\psi_k^*(\mathbf{x},\tau)}{\gamma}, \tag{A3}$$

where β is an offset factor chosen so that its magnitude is above the magnitude of the aquifer bottom elevation and river bottom elevation, and γ is a scaling factor chosen so that magnitudes of modified initial conditions (shown below) are large relative to the offset factor β to avoid truncation errors. We found that values of $\gamma \approx 10^{-8} - 10^{-6}$ are adequate in most cases.

[60] With the change of variables in (A1)–(A3), the adjoint equations (21)–(23) become

$$S_y \frac{\partial \Psi_u^*}{\partial \tau} = \nabla \cdot \left[\mathbf{K}(h_{uo} - \zeta)\nabla \Psi_u^*\right] - \frac{K_a}{b_a}\left(\Psi_u^* - \Psi_c^*\right) + \sum_{k=1}^{N} \frac{K_k}{b_k}\left(\Psi_k^* - \Psi_u^*\right) B_k(\mathbf{x}) - \frac{E_{Tmax}}{d}\left(\Psi_u^* - \beta\right)\left[H(h_u - h_s + d) - H(h_u - h_s)\right] \tag{A4}$$

$$S \frac{\partial \Psi_c^*}{\partial \tau} = \nabla \cdot \left[\mathbf{T}\nabla \Psi_c^*\right] + \frac{K_a}{b_a}\left(\Psi_u^* - \Psi_c^*\right) \tag{A5}$$

$$-\frac{\partial}{\partial s_k}\left[\frac{5c}{3}\frac{S_{ok}^{1/2} w_k}{n_k}\left(h_{ko} - z_k\right)^{2/3}\Psi_k^*\right] = -\frac{K_k}{b_k}\left(\Psi_k^* - \Psi_u^*\right) w_k - \Psi_k^* \frac{\partial}{\partial s_k}\left[\frac{5c}{3}\frac{S_{ok}^{1/2} w_k}{n_k}\left(h_k - z_k\right)^{2/3}\right] \text{for } k = 1, 2, \ldots N, \tag{A6}$$

[61] The boundary and initial conditions for these adjoint states are

$$\Psi_u^*(\mathbf{x},\tau) = \beta \text{ on } \Gamma_{1u}, \tag{A7}$$

$$\nabla \Psi_u^* \cdot \mathbf{n} = 0 \text{ on } \Gamma_{2u}, \tag{A8}$$

$$\alpha_u \Psi_u^*(\mathbf{x},\tau) - \mathbf{K}\nabla \Psi_u^* \cdot \mathbf{n} = \alpha_u \beta \text{ on } \Gamma_{3u}, \tag{A9}$$

$$\Psi_c^*(\mathbf{x},\tau) = \beta \text{ on } \Gamma_{1c}, \tag{A10}$$

$$\nabla \Psi_c^* \cdot \mathbf{n} = 0 \text{ on } \Gamma_{2c}, \tag{A11}$$

$$\alpha_c \Psi_c^*(\mathbf{x},\tau) - \mathbf{T}\nabla \Psi_c^* \cdot \mathbf{n} = \alpha_c \beta \text{ on } \Gamma_{3c}, \tag{A12}$$

$$\Psi_N^*(s_N = L_N, \tau) = \beta, \tag{A13}$$

$$\Psi_k^*(s_k = L_k, \tau) = \Psi_{d_k}^*(s_{d_k} = 0, \tau) \qquad \text{for } k = 1, 2, \ldots N-1. \tag{A14}$$

$$\Psi_u^*(x, y, \tau = 0) = \beta + \sum_{k=1}^{N} \frac{K_k}{b_k S_y \gamma} B_k(\mathbf{x}) \tag{A15}$$

$$\Psi_c^*(x, y, \tau = 0) = \beta \tag{A16}$$

[62] With this change of variables, stream depletion is calculated as

$$\Delta Q_N(L_N, \tau = 0) = \Delta Q_N(L_N, t = t_c) \approx Q_{pj} \int_0^{t_c} \gamma\left[\Psi_j^*(\mathbf{x},\tau) - \beta\right] d\tau, \tag{A17}$$

for pumping from a well at any location $\mathbf{x}$ in aquifer j ($j = u$ for unconfined, $j = c$ for confined).

[63] A modified version of the Stream (STR) package of MODFLOW was developed to solve the adjoint equation (23) (see *Griebling* [2012] for more information). The adjoint equations can be solved using MODFLOW with this modified STR package, for user-selected values of β and γ. The simulated "head" in the unconfined aquifer and confined aquifers represent Ψ_u^* and Ψ_c^*, respectively. These values are used in equation (A17) to calculate stream depletion.

[64] **Acknowledgments.** We thank four anonymous reviewers, the associate editor, and the editor for valuable comments on this manuscript. This work was funded by the National Institutes for Water Resources, under Project 2009CO195G.

References

Butler, J. J., V. A. Zlotnik, and M. -S. Tsou (2001), Drawdown and stream depletion produced by pumping in the vicinity of a partially penetrating stream, *Ground Water*, *39*(6), 651–659.

Butler, J. J., X. Zhan, and V. A. Zlotnik (2007), Pumping-induced drawdown and stream depletion in a leaky aquifer system, *Ground Water*, *45*(2), 178–186.

Deutsch, C., and A. Journel (1992), *GSLIB: Geostatistical Software Library and User's Guide*, Oxford Univ. Press, New York.

Glover, R. E., and G. G. Balmer (1954), River depletion resulting from pumping a well near a river, *Trans. AGU*, *35*, 468–470.

Griebling, S. A. (2012), *Quantification of Stream Depletion due to Aquifer Pumping Using Adjoint Methodology*, MS thesis, Univ. Colo. Boulder, Boulder, Colo.

Hantush, M. S. (1965), Wells near streams with semipervious beds, *J. Geophys. Res.*, *70*(12), 2829–2838.

Harbaugh, A. W., E. R. Banta, M. C. Hill, and M. G. McDonald (2000), MODFLOW-2000, the U.S. Geological Survey modular ground-water model—User guide to modularization concepts and the ground-water flow process, U.S. Geol. Surv. Open File Rep. 00–92, Reston, Va.

Hunt, B. (1999), Unsteady stream depletion from groundwater pumping, *Ground Water*, *37*(1), 98–102.

Hunt, B. (2009), Stream depletion in a two-layer leaky aquifer system, *J. Hydrol. Eng.*, *14*(9), 895–903.

Jenkins, C. T. (1968), Techniques for computing rate and volume of stream depletion by wells, *Ground Water*, *6*(2), 37–46.

Lambert, P. M., T. Marston, B. A. Kimball, and B. J. Stolp (2011), Assessment of groundwater/surface-water interaction and simulation of potential streamflow depletion induced by groundwater withdrawal, Uinta river near Roosevelt, Utah, U.S. Geol. Surv. Sci. Invest. Rep. 2011–5044, Reston, Va.

Leake, S. A., and D. R. Pool (2010), Simulated effects of groundwater pumping and artificial recharge on surface-water resources and riparian vegetation in the Verde valley sub-basin, central Arizona, U.S. Geol. Surv. Sci. Invest. Rep. 2010–5147, Reston, Va.

Leake, S. A., J. P. Hoffmann, and J. E. Dickinson (2005), Numerical ground-water change model of the c aquifer and effects of ground-water withdrawals on stream depletion in selected reaches of clear creek, Chevelon creek, and the little Colorado river, northeastern Arizona, U.S. Geol. Surv. Sci. Invest. Rep. 2005–5277, Reston, Va.

Leake, S. A., H. W. Reeves, and J. E. Dickinson (2010), A new capture fraction method to map how pumpage affects surface water flow, *Ground Water*, *48*(5), 690–700.

Myers, N. C., X. Jian, and G. D. Hargadine (1996), Effects of pumping municipal wells at Junction city, Kansas, on streamflow in the Republican river, northeast Kansas, 1992–94, U.S. Geol. Surv. Water Resour. Invest. Rep. 96–4130, Reston, Va.

Neupauer, R. M., and S. A. Griebling (2012), Adjoint simulation of stream depletion due to aquifer pumping, *Ground Water*, *50*, 746–753, doi:10.1111/j.1745–6584.2011.00901.x.

Peterson, S. M., J. S. Stanton, A. T. Saunders, and J. R. Bradley (2008), Simulation of ground-water flow and effects of ground-water irrigation and base flow in the Elkhorn and Loup river basins, Nebraska, U.S. Geol. Surv. Sci. Invest. Rep. 2008–5143, Reston, Va.

Prudic, D. E. (1989), Documentation of a computer program to simulate stream-aquifer relations using a modular, finite-difference, ground-water flow model, U.S. Geol. Surv. Open File Rep. 88–729, Reston, Va.

Sophocleous, M., A. Koussis, J. L. Martin, and S. P. Perkins (1995), Evaluation of simplified stream-aquifer depletion methods for water rights administration, *Ground Water*, *33*(4), 579–588.

Stanton, J. S., S. M. Peterson, and M. N. Fienen (2010), Simulation of groundwater flow and effects of groundwater irrigation on stream base flow in the Elkhorn and Loup river basins, Nebraska, 1895–2055, Phase Two, U.S. Geol. Surv. Sci. Invest. Rep. 2010–5149, Reston, Va.

Theis, C. V. (1941), The relation between the lowering of the piezometric surface and the rate and duration of discharge of a well using groundwater storage, *Trans. AGU*, *22*, 734–738.

Wallace, R. B., Y. Darama, and M. D. Annable (1990), Stream depletion by cyclic pumping of wells, *Water Resour. Res.*, *26*, 1263–1270.

Zlotnik, V. A., and D. M. Tartakovsky (2008), Stream depletion by groundwater pumping in leaky aquifers, *J. Hydrol. Eng.*, *13*(2), 43–50.